PCCP

Accepted Manuscript

ROYAL SOCIETY OF CHEMISTRY

www.rsc.org/pccp

Cite this: DOI: 10.1039/c0xx00000x

www.rsc.org/xxxxxx

PAPER

Growth of Axial Nested P-N Heterojunction Nanowires for High Performance Diode

Nan Chen, Zheng Xue, Hui Yang, Zhou Zhang, Juan Gao, Yongjun Li and Huibiao Liu*

Received (in XXX, XXX) Xth XXXXXXXXX 20XX, Accepted Xth XXXXXXXXX 20XX

DOI: 10.1039/b000000x

Heterojunction nanomaterials have attracted the interests of a broad range of scientists and engineers to explore fundamental scientific understanding the formation of heterojunction nanostructure, special properties with enhanced electrical and optical performance and the relationship between functionality and molecule structures. In this work, we synthesized a novel axial nested P-N heterojunction nanowire combined inorganic semiconductor PbS and organic conjugated polymers polypyrrole (PPy). The nested P-N heterojunction nanowires (NWs) show higher rectification ratio (exceeded 100), long-term stability and high unilateral conductivity due to the producing bigger area of junction.

Introduction

Low-dimensional nanoscale materials have attracted more attention for some technological applications that can be derived from their peculiar and fascinating properties.[1-8] Recently, some research has focused on P-N heterojuntion nanomaterials, because their unique electronic properties especially, integration performance suggest great potential for electronic applications.[9-22] It is known that the P-N heterojunctions are of great importance in modern electronic applications, which always showed unique properties, particularly optical, electrical and photoelectrical. Low dimension inorganic/organic hybrids as P-N junctions of nanostructures, which are combination of functional organic and inorganic moieties to produce a new class inorganic/organic solid materials with distinct structure.[23] Lead sulfide (PbS) is an important direct band gap semiconductor material with a rather small bulk band gap of 0.41 eV at 300 K [24] and strong quantum confinement effect owing to its large Bohr radius (*ca*. r_B=18 nm) [25-27] that has applications in electronic devices,[28-30] photovoltaic,[31] optoelectronic devices,[32] mid-infrared lasers,[33, 34] and thermoelectrics [35, 36]. Moreover, a great deal of work has been devoted to the synthesis of PbS nanostructures with tunable size in diverse methods including nanowires,[37, 38] nanorods,[39] nanobelts,[40] nanocubes,[41] nanodendritic,[42, 43] and nanocrystals. [44, 45] These nanoarchitectures have been employed as important nanoscale building blocks for advanced materials and smart miniature devices to fulfill the increasing needs of high materials usage efficiency. The conducting π-conjugated organic polymers have been intensively studied for their excellent electrical and photoelectrical properties.[46] In general, the conjugated polymers are referred to as organic semiconductors with "intrinsic wide band gap semiconductors" down to "insulators" with a negligibly low intrinsic charge carrier density in their neutral states.[1, 2] The π-conjugated polymer-based functional organic nanomaterials are considered to be good candidates for the next generation miniature electronic devices. Among these π-conjugated polymers, polypyrrole (PPy) is one of the most investigated due to its high electrical conductivity and its easily prepared.[47]

The area of junction is the most important factor for improving the property of heterojunction. The electronic property will be obviously promoted with increasing the area of heterojunction. [9-22] The hard-template synthesis employs a physical template such as anodized alumina oxide as a scaffold for the growing nanostructures of conducting polymers. The target material was first precipitated in the template by the electrochemical deposition method. We used ordered porous anodized alumina oxide (AAO) templates and chose the N-type inorganic semiconductor of PbS and P-type organic semiconductor of PPy to prepare heterojunction NWs because of their matched energy levels (Figure S1).[12, 41] In this work, we developed a special strategy to control synthesis a novel axial nested P-N heterojunction nanowires based inorganic semiconductor PbS and organic conjugated polymers PPy by electrochemical deposition method with the help of AAO templates. The axial nested P-N heterojunction NWs show bigger area of junction than that of axial planar heterojunction nanowires. As we expected, the electrical properties of axial nested P-N heterojunction NWs exhibited a higher rectification ratio and conductivity, which is comparing to other heterojunction nanowires. [48-51]

Experimental Section

Materials. Lithium perchlorate ($LiClO_4$) were purchased from Aldrich Corp. lead(II) chloride, sublimed sulfur, dimethyl sulfoxide (DMSO), pyrole, acetonitrile and acetone were purchased from Beijing Chemical reagent Corporation, China. All of the reagents were used as received. The anodic aluminum oxide (AAO) templates with porous diameter of 200 nm and a thickness of 60 μm were purchased from Whatman Co. The NWs were synthesized by a homemade electoral cell. All chemicals used in this work were used as received.

Synthesis of PbS-PPy heterojunction nanowires (NWs). Firstly sputtered a layer of Au with 100 nm of thickness on one side of

the AAO template as conducting layer, and then put the AAO template into a homemade electrolytic cell as working electrode and an saturated calomel electrode (SCE) reference electrode in a three-electrode electrochemical cell. PbS NWs were deposited into the AAO template at a current density of 2.0 mA/cm^2 in a DMSO solution consisted of 28 mM $PbCl_2$ and 95 mM element sulfur at the temperature of about 115 °C for 5400 s. After deposition, the as-prepared samples were taken out, and rinsed with hot DMSO and acetone for several times, respectively, then dried in air at room temperature. In the following electrodeposition process of PPy: PPy deposition was carried out from a 0.1 M pyrole and 0.1 M $LiClO_4$ acetonitrile solution by applying a suitable voltage for an appropriate time next (typically 50 min). Finally, the PbS-PPy heterojunction NWs embedded AAO membrane was prepared. The AAO template was selectively etched by NaOH solution (2 M) and cleaned by deionized water several times for chareacteriaztion and measurement.

Characterization. Field emission scanning electron microscopy (SEM) images and energy-dispersive X-microanalysis spectrum (EDS) were taken from Hitachi S-4800 FESEM microscope at an accelerating voltage of 5 kV and 15 kV. Transmission electron microscopy (TEM) images and selective-area electron diffraction pattern (SAED) were taken from JEOL JEM-1011 and 2011 microscope at an accelerating voltage of 100 kV. The FIB PbS-PPy heterojunction nanodevices were performed on a FEI FIB/SEM Nova 200 NanoLab UHR FEG. Electroproperty of devices was recorded with a Keithley 4200 SCS in a clean and shielded box at room temperature in air.

Results and Discussion

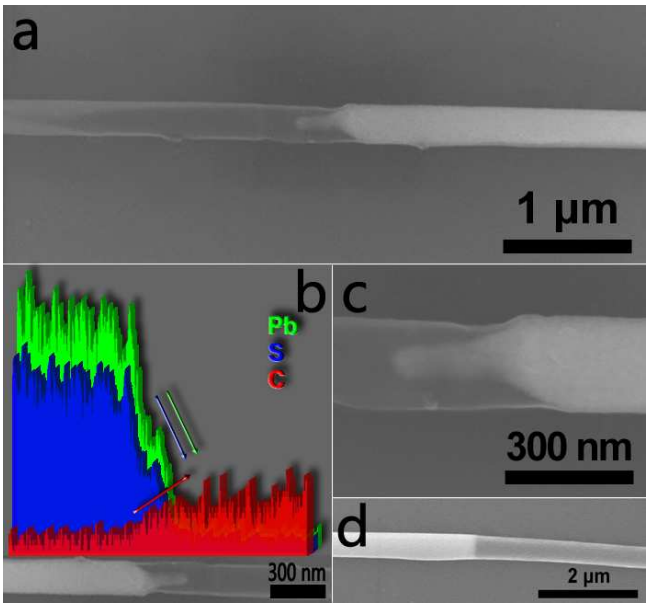

Figure 1. SEM image of PbS-PPy axial nested P-N heterojunction NW (a); the linear scanning of a single PbS-PPy NW (b); nested P-N junction of PbS-PPy heterojunction NW under a large magnification (c).

As-synthesized PbS-PPy heterojunction NW was characterized by SEM. **Figure 1a** shows a single PbS-PPy heterojunction NW on silicon at lower magnification. The diameter of PbS-PPy heterojunction NW was about 270 nm with a smooth surface. The area of heterojunction could be calculated from the equation $S = \pi R (L^2 + R^2)^{1/2}$, where R, L and S is the radius (i.e. 270 nm), length and area of the heterojunction, respectively. The length of p-n heterojunction is up to 450 nm and the area of heterojunction is at least 0.44 μm^2, which is 14 times of the area of axial planar heterojunction. In **Figure 1c**, comparing the axial planar P-N junction,[14] the axial nested P-N junction showed a not clear interface between inorganic and organic materials. The right dark side is organic semiconductor PPy, and the other part is inorganic molecular of PbS. The results were further confirmed by the EDS analysis in **Figure 1b**, in which lead, sulfur, and carbon element changed gradually near the nested P-N heterojunction indicating that, unlike the connected head to head in axial planar P-N heterojunction, the contact surface of both inorganic and organic materials was significantly greater than the cross-section of the NWs.

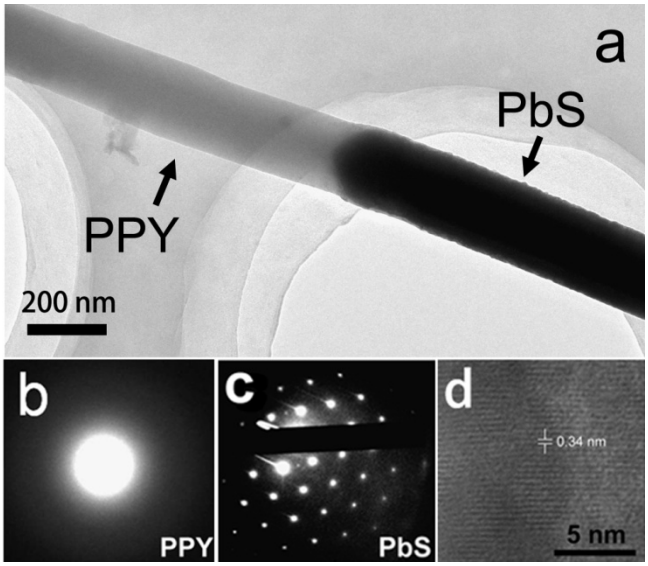

Figure 2. TEM image of several nested P-N junction PbS-PPy heterojunction NWs (a), and SAED taken from segment in the NW of organic and inorganic parts (b and c); HRTEM image of PbS, the fringes are separated by 0.34 nm (d).

For transmission electron microscopy (TEM) characterization, **Figure 2a** clearly shows the wire-like nanostructure. The inorganic/organic nested P-N junction formed by inorganic semiconductor and organic semiconducting can be clearly observed. The selective-area electron diffraction pattern (SAED) pattern has been shown in Figure 2b-c, which shows that the bright part is amorphous PPy, and the dark part is polycrystal characteristic PbS (as shown in **Figure 2c** and **2d**). The fringes are separated by 0.34 nm, corresponding to the interplanar distance between {111} facets as shown in **Figure 2d**. It is well-known that the [111] HRTEM image of the face-center cubic (*fcc*) crystal is built by 3 sets of the {220} spacing with a 6-fold symmertry.[52] The typical image of the single PbS-PPy heterojunction NW with a diameter about 270 nm, which agrees with the SEM images well. The axial nested P-N junction in the TEM image has significant difference compared with the axial planar P-N junction.

Figure 3a is the X-ray diffraction (XRD) pattern of the as-prepared PbS (top, Purple) that shows a degree of crystallinity. All of the peaks is in agreement with the standard data from Bragg reflections of the standard *fcc* structure of PbS (space group: *Fm3m* (225), a=0.5936 nm, JCPDF # 05-0592) (bottom, green).[53] First, the preferential growth along the different directions leads to the formation of various PbS nanostructures. It is worth noting that the ratio between the intensities of the (200) and (111) diffraction peaks is much higher than the conventional value (1.30 vs 1.19), which indicates that PbS NW may be abundant in {111} facets (as shown in Figure 3b), and thus lead to relatively greater accelerated growth along the (111) face leading to the formation of cone non-planar tip NW as shown **Figure 3c** (I).

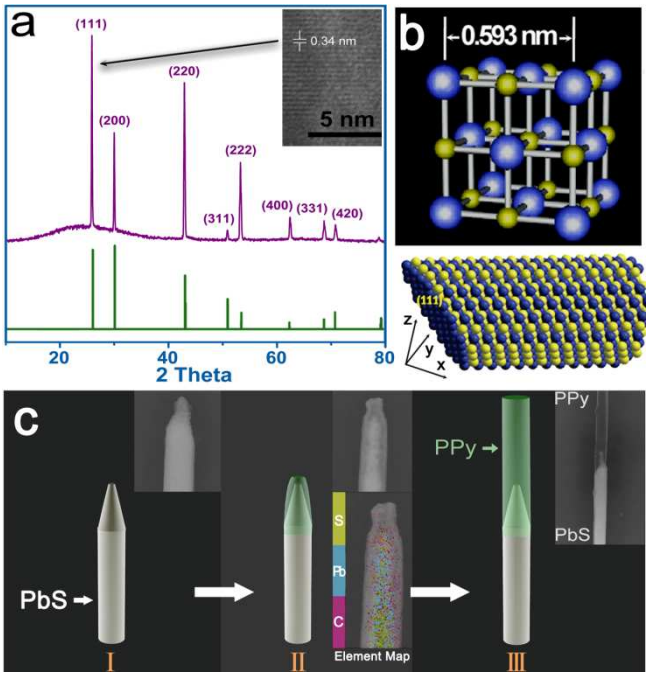

Figure 3. X-ray diffraction (XRD) pattern of the as-prepared PbS NW, 2 theta and fringes data: (111), 25.9°, 0.34 nm; (200), 30.0°, 0.29 nm; (220), 42.9°, 0.21 nm; (311), 50.9°, 0.18 nm; (222), 53.3°, 0.17 nm; (400), 62.4°, 0.15 nm; (331), 68.7°, 0.14 nm; (420), 70.8°, 0.13 nm, as well as the standard data (green) for PbS (JCPDS 05-0592) (a); ball-and-stick model of cubic rock salt PbS structure (blue and yellow represents lead and sulfur atoms, respectively (up), indexed facets (111) of PbS rock-salt structure (down) [54] (b); progress on preparation of nested P-N junction PbS-PPy heterojunction NW (c).

When it comes to the formation of axial nested heterojunction between PbS and PPy. As an interesting result, in more detail with respect to the "how" the organic component is incorporated in the cone non-planar surface of PbS. The major advantage of PPy moieties over the PbS molecular materials alone is based on the coordination ability and increase in non-planar active surface area to form good electronic contact between the inorganic and organic components. Specifically, PPy NW wrapped up the cone tip of PbS NW in AAO template by electrochemical deposition under an appropriate current density for some time. The SEM image in **Figure 3c** (II) showed that PPy just wrapped around PbS NW, the light part in the center of this NW was PbS while the outside dark thin layer is PPy. The results were consistent with elements map as shown in **Figure 3c** (II); Finally, with the growth of PPy a well-defined P-N heterojunction NW has formed as shown in **Figure 3c** (III).

The device of PbS-PPy heterojunction NW was measured with a Keithly 4200 SCS semiconductor characterization system and a shielded probe station with triax connectors to minimize noise at room temperature. FIB/SEM System has been playing an important role in the construction of PbS-PPy heterojunction NW device, Pt metal is chosen as the electrodes for electrical characterization that was made by Focus Ion Beam (FIB) method. The device structure consisting of PbS-PPy heterojunction NW is shown in **Figure 4a**. Our investigation shows that the Current (*I*) *versus* Voltage (*V*) characteristics of the PbS-PPy NW clearly reveal stable rectifying diode behavior, which exhibits a high rectification ratio (I_F/I_R) is greater than 100 at 15 V, and rectifying behavior for the device with turn-on voltage is observed at about 5 V under forward bias and relatively small leakage current as shown in **Figure 4b**. Furthermore, the rectification ratio of the diode is easy to learn from the inset in **Figure 4b**. A high rectification ratio implies better combination of nested P-N junction between the n-type inorganic semiconductor PbS and p-type organic polymer PPy than ordinary planar P-N junction. Experimentally, PbS-PPy NW shows very high current of above 60 μA in dark with forward applied bias of 15 V for both majority holes and majority electrons can flow through the p-n junction and contribute to the forward current, while the current transporting through the junction of NW arrays in reverse bias at reverse bias at -15 V bias is less than 1 μA, because neither majority holes nor majority electrons can flow through the p-n junction at reverse bias. Compared to the previous similar research,[48-50] the conductivity and rectification ratio of PbS-PPy heterojunction NW diode can emulate some inorganic materials.[55]

The PbS-PPy nested P-N nanowires from the designed the route of self-assembly showed good contacting between organic polymer and inorganic and improved the physical properties due to the bigger area of heterjunction resulting in stronger interaction on interface. Both the maximum current through the P-N junction and breakdown voltage actually depend on the heterjunction areas.[56-59] As we know that, long-term stability that has yet to be demonstrated will also be a common problem for many of the NW-based devices.[60] However, the performance of axial nested PbS-PPy of NW in the nanodiode device is good enough and show good electrical stability, as shown in **Figure 4c**, the high similar capacity of the conductivity curve that tested for many times indicates that PbS-PPy axial nested P-N junction heterojunction NW is stable in diode character. The advantage on electrics of the nested P-N heterojunction wire show obvious improvement due to the bigger area heterjunction resulting in strong junction effects in the nanowires.

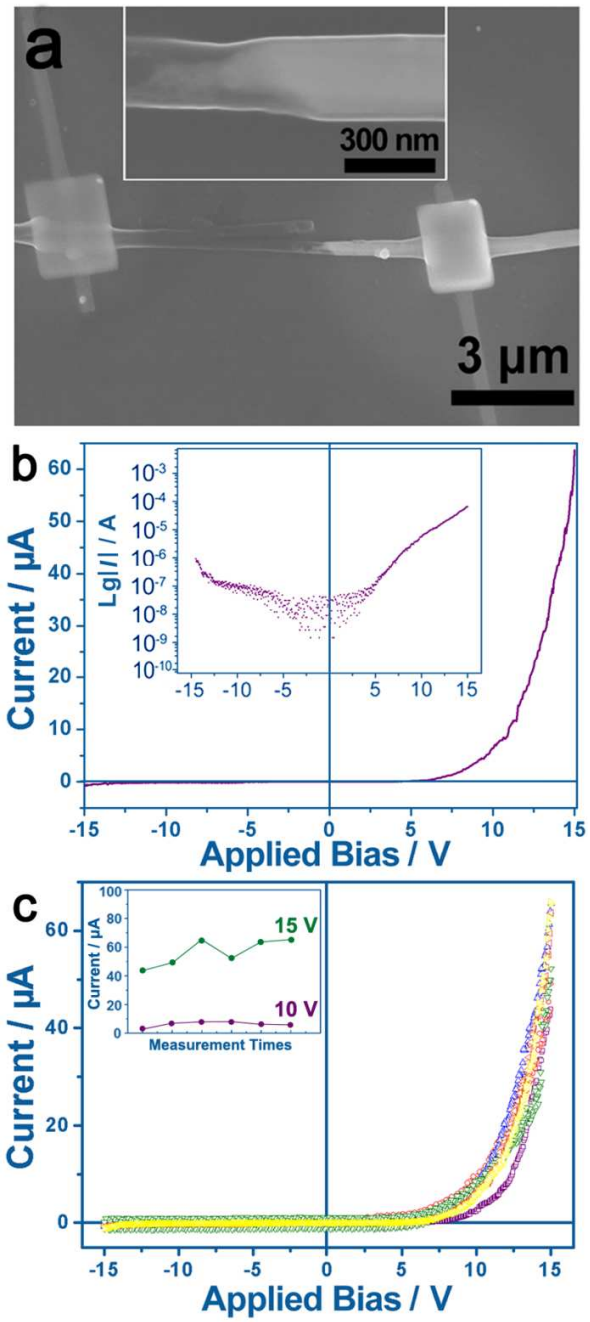

Figure 4. SEM image of a single PbS-PPy nested P-N junction heterojunction NW device made by FIB (a); Typical current-voltage (*I-V*) curves for a single PbS-PPy heterojunction NW at room temperature in the dark (inset: semilog plot of the same data used to extract the diode rectification) (b); conductivity stability of a single diode PbS-PPy heterojunction NW at room temperature has been tested for many times (different colors), (inset: current stability test under selected bias) (c).

Conclusions

A novel axial nested P-N heterojunction nanostructure was designed and synthesized which combine inorganic semiconductor PbS and conducting polymers PPy, in which the area of junction is up to 0.44 μm^2. The advantage on electrics of the axial nested P-N heterojunction nanowires show obvious improvement due to the bigger area of heterjunction leading to junction effects. Compared with the axial planar P-N heterojunction NWs, the axial nested P-N heterojunction nanowires show a higher rectification ratio (greater than 100), as well as the conductivity. We believe that, the long-term stability, high unilateral conductivity of PbS-PPy nested P-N heterojunction NW will make it more suitable as some of the key parts in nanodevices.

Notes and references

CAS Key Laboratory of Organic Solids, Beijing National Laboratory for Molecular Sciences (BNLMS), Institute of Chemistry, Chinese Academy of Sciences, Beijing, 100190, P. R. China. Fax: 861082616576X; Tel: 861082615870; E-mail: liuhb@iccas.ac.cn

† Electronic Supplementary Information (ESI) available: The energy level diagram of PbS and PPy. See DOI: 10.1039/b000000x/

‡ This work was supported by the National Basic Research 973 Program of China (2011CB932302 and 2011CB932303) and the National Nature Science Foundation of China (21031006, 21373235 and 91227113).

1 W. Lu, J. Xiang, B. Timko, Y. Wu and C. M. Lieber, *PNAS* **2005**, *102*, 10046.
2 F. Léonard and A. A. Talin, *Nat. Nanotechnol.* **2011**, *6*, 773.
3 Y. Li, T. Liu, H. Liu, M. Tian and Y. Li, *Acc. Chem. Res.* **2014**, *47*, 1186.
4 A. Balandin, *Nat. Mater.* **2011**, *10*, 569.
5 N. Chen, C. Huang, W. Yang, S. Chen, H. Liu, Y. Li and Y. Li, *J. Phys. Chem. C*, **2010**, *114*, 12982.
6 J. Xiao, B. Yang, J. Wong, Y. Liu, F. Wei, K. Tan, X. Teng, Y. Wu, L. Huang, C. Kloc, F. Boey, J. Ma, H. Zhang, H. Yang and Q. Zhang, *Org. Lett.* **2011**, *13*, 3004.
7 Y. Liu, F. Boey, L. Lao, H. Zhang, X. Liu and Q. Zhang, *Chem. - Asian J.* **2011**, *6*, 1004.
8 B. Yang, J. Xiao, J. Wong, J. Guo, Y. Wu, L. Ong, L. Lao, F. Boey, H. Zhang, H. Yang and Q. Zhang, *J. Phys. Chem. C* **2011**, *115*, 7924.
9 H. Liu, J. Xu, Y. Li and Y. Li, *Acc. Chem. Res.* **2010**, *43*, 1496.
10 H. Zheng, Y. Li, H. Liu, X. D. Yin and Y. Li, *Chem. Soc. Rev.* **2011**, *40*, 4506.
11 S. Cui, H. Liu, L. Gan, Y. Li and D. Zhu, *Adv. Mater.* **2008**, *20*, 2918.
12 X. Qian, H. Liu and Y. Li *Chin. Sci. Bull.* **2013**, *58*, 2686.
13 J. Xiao, Z. Yin, Y. Wu, J. Guo, Y. Cheng, H. Li, Y. Huang, Q. Zhang, J. Ma, F. Boey, H. Zhang and Q. Zhang, *Small* **2011**, *7*, 1242.
14 Y. Guo, Q. Tang, H. Liu, Y. Zhang, Y. Li, W. Hu, S. Wang and D. Zhu, *J. Am. Chem. Soc.* **2008**, *130*, 9198.
15 Y. Guo, H. Liu, Y. Li, G. Li, Y. Zhao, Y. Song and Y. Li, *J. Phys. Chem. C* **2009**, *113*, 12669.
16 Y. Guo, Y. Zhang, H. Liu, S. Lai, Y. Li, Y. Li, W. Hu, S. Wang, C. Che and D. Zhu, *J. Phys. Chem. Lett.* **2010**, *1*, 327.
17 H. Lin, H. Liu, X. Qian, C. Ouyang and Y. Li, *Dalton Trans.* **2011**, *40*, 4397.
18 N. Chen, X. Qian, H. Lin, H. Liu, Y. Li and Y. Li, *Dalton Trans*. **2011**, *40*, 10804.
19 H. Lin, H. Liu, X. Qian, S.-W. Lai, Y. Li, N. Chen, C. Ouyang, C.-M. Che and Yuliang Li, *Inorg. Chem.* **2011**, *50*, 7749.
20 N. Chen, S. Chen, C. Ouyang, Y. Yu, T. Liu, Y. Li, H. Liu and Y. Li, *NPG Asia Materials* **2013**, *5*, e59.
21 H. Lin, H. Liu, X. Qian, S. Chen, Y. Li and Y. Li, *Inorg. Chem.* **2013**, *52*, 6969.
22 K. Wang, X. Qian, L. Zhang, Y. Li and H. Liu, *ACS Appl. Mater. Interfaces* **2013**, *5*, 5825.
23 P. Gomez, *Adv. Mater.* **2001**, *13*, 163.
24 P. Hoyer, R and Könenkamp, *Appl. Phys. Lett.* **1995**, *66*, 349.
25 F. Wise, *Acc. Chem. Res.* **2000**, *33*, 773.
26 J. Machol, F. Wise, R. Patel and D. Tanner, *Phys. Rev. B* **1993**, *48*, 2819.
27 N. Zhao and L. Qi, *Adv. Mater.* **2006**, *18*, 359.
28 J. Pijpers, R. Ulbricht, K. Tielrooij, A. Osherov, Y. Golan, C. Delerue, G. Allan and M. Bonn, *Nat. Phys.* **2009**, *5*, 811.

29 R. Graham, C. Miller, E. Oh and D. Yu, *Nano Lett.* **2011**, *11*, 717.
30 N. Chen, X. Qian, H. Lin, H. Liu and Y. Li, *J. Mater. Chem.* **2012**, *22*, 11068.
31 K. Acharya, N. Hewa-Kasakarage, T. Alabi, I. Nemitz, E. Khon, B. Ullrich, P. Anzenbacher and M. Zamkov, *J. Phys. Chem. C* **2010**, *114*, 12496.
32 R Joshi, A. Kanjilal and H. Sehgal, *Appl. Surf. Sci.* **2004**, *221*, 43.
33 M. Neo, N. Venkatram, G. Li, W. Chin and W. Ji, *J. Phys. Chem. C* **2010**, *114*, 18037.
34 F. Tittel, D. Richter and A. Fried, *Top. Appl. Phys.* **2003**, *89*, 458.
35 J. Androulakis, C. Lin, H. Kong, C. Uher, C. Wu, T. Hogan, B. Cook, T. Caillat, K. Paraskevopoulos and M. Kanatzidis, *J. Am. Chem. Soc.* **2007**, *129*, 9780.
36 Y. Lin and M. Dresselhaus, *Phys. Rev. B* **2003**, *68*, 075304.
37 M. Bierman, Y. Albert, A. Kvit, A. Schmitt and S. Jin, *science* **2008**, *320*, 1060.
38 Y. Albert, D. Chernak, M. Bierman and S. Jin, *J. Am. Chem. Soc.* **2009**, *131*, 16461.
39 J. Wan, X. Chen, Z. Wang, W. Yu and Y. Qian, *Mater. Chem. Phys.* **2004**, *88*, 217.
40 L. Dong, Y. Chu, Y. Liu, M. Li, F. Yang and L. Li, *J. Colloid. Interf. Sci.* **2006**, *301*, 503.
41 G. Zhou, M. Lu, Z. Xiu, S. Wang, H. Zhang, Y. Zhou and S. Wang, *J. Phys. Chem. B* **2006,** *110,* 6543.
42 S. Lee, Y. Jun, S. Cho and J. Cheon, *J. Am. Chem. Soc.* **2002**, *124*, 11244.
43 D. Kuang, A. Xu, Y. Fang, H. Liu, C. Frommen and D. Fenske, *Adv. Mater.* **2003**, *15*, 1747.
44 M. Jones, K. Osberg, R. Macfarlane, M. Langille and C. Mirkin, *Chem. Rev.* **2011**, *111*, 3736.
45 J. Joo, H. Na, T. Yu, J. Yu, Y. Kim, F. Wu, J. Zhang and T. Hyeon, *J. Am. Chem. Soc.* **2003**, *125*, 11100.
46 K. Ramanathan, M. Bangar, M. Yun, W. Chen, N. Myung and A. Mulchandani, *J. Am. Chem. Soc.* **2005**, *127*, 496.
47 Y. Berdichevsky and Y. Lo, *Adv. Mater.* **2006**, *18*, 122.
48 A. Kumar and A. Jakhmola, *J Colloid Interf. Sci.* **2006**, *297*, 607.
49 Y. Huang, X. Duan, Y. Cui, L. Lauhon, K. Kim and C. Lieber, *Science* **2001**, *294*, 1313.
50 E. Tutuc, J. Appenzeller, M. Reuter and S. Guha, *Nano Lett.* **2006**, *6*, 2070.
51 K. Peng, Z. Huang and J. Zhu, *Adv. Mater.* **2004**, *16*, 73.
52 B. Tian, X. Zheng, T. Kempa, Y. Fang, N. Yu, G. Yu, J. Huang and C. Lieber, *Nature* **2007**, *449*, 885.
53 S. Kundu, J. Hill, G. Richards, K. Ariga, A. Khan, U. Thupakula and S. Acharya, *ACS Appl. Mater. Inter.* **2010**, *2*, 2759.
54 N. Wang, X. Cao, L. Guo, S. Yang and Z. Wu, *ACS nano* **2008**, *2*, 184.
55 V. Germain, J. Li, D. Ingert, Z. Wang and M. Pileni, *J. Phys. Chem. B* **2003**, *107*, 8717.
56 T. Lee, W. Choi, J. Kar, Y. Kang, J. Jeon, J. Park, Y. Kim, H. Baik and J. Myoung, *Nano Lett.* **2010,** *10*, 3517.
57 M. Choi, D. Qu, D. Lee, X. Liu, K. Watanabe, T. Taniguchi, W. Yoo, ACS Nano, 2014, 8, 9332.
58 P. Nirmalraj, A. Bellew, A. Bell, J. Fairfield, E. McCarthy, C. Kelly, L. Pereira, S. Sorel, D. Morosan, J. Coleman, M. Ferreira, J. Boland, Nano Lett., 2012, 12, 5966.
59 K.l Mohanta , S. Batabyal, A. Pal, Chem. Mater., 2007, 19, 3662.
60 P. Yang, R. Yan and M. Fardy, *Nano Lett*. **2010**, *10*, 1529.